



ACADEMIC  
PRESS

Available online at [www.sciencedirect.com](http://www.sciencedirect.com)

SCIENCE @ DIRECT®

Journal of Magnetic Resonance 164 (2003) 358–364

JMR

Journal of  
Magnetic Resonance

[www.elsevier.com/locate/jmr](http://www.elsevier.com/locate/jmr)

Communication

## Transient oscillations under strongly mismatched Hartmann–Hahn conditions

Zoran D. Žujović,<sup>a,\*</sup> Graham A. Bowmaker,<sup>a</sup> and Christian Mayer<sup>b</sup>

<sup>a</sup> Department of Chemistry, The University of Auckland, Private Bag 92019, Auckland, New Zealand

<sup>b</sup> Institut für Physikalische und Theoretische Chemie, Universität Duisburg, Duisburg 47048, Germany

Received 27 March 2003; revised 11 July 2003

### Abstract

Based on the standard 2D Polarization inversion experiment, a new pulse sequence (PI-TAPF) is proposed. It represents a combination of Polarization Inversion and TAPF (time averaged precession frequency) sequences. The depolarization period consists of phase-alternating intervals of different duration in the *I* channel. The pulse sequence yields transient oscillations under the strongly mismatched HH conditions where the required power for the dilute spins is reduced by a factor of 5. Experimental results recorded for a sample of ferrocene powder are well reproduced by numerical simulations.

© 2003 Elsevier Inc. All rights reserved.

**Keywords:** Cross polarization; Transient oscillations; Polarization inversion; Mismatching; Spin exchange

### 1. Introduction

Heteronuclear cross polarization (CP) experiments are of great practical importance for the signal enhancement of low- $\gamma$  nuclear spins [1–3]. Polarization of high- $\gamma$  spins (*I*) is transferred to the low- $\gamma$  (*S*) spins by simultaneous irradiation of both spins with two resonant RF fields. Optimum transfer is achieved for equal nutation frequencies of the *I* and *S* spins about the applied RF fields, i.e., when the Hartmann–Hahn matching condition,  $|\gamma_I B_{1I}| = |\gamma_S B_{1S}|$ , is fulfilled.

In general, there are two types of CP dynamics [3–5]. For an abundant spin system with strong internal interactions, the polarization transfer can be described by thermodynamic picture that leads to an exponential dependence of the magnetization as a function of contact time. However, in the case of strong coupling between directly coupled *I*–*S* spins the cross-polarized magnetization evolves in a damped oscillatory fashion, especially near the Hartmann–Hahn match. The damping of the oscillations is caused by interactions of directly coupled *I*–*S* spin pairs with neighboring

protons. This phenomenon, called transient oscillations (TO), was detected by Müller et al. [6] in Hartmann–Hahn cross-polarization experiments on a single crystal of ferrocene and has been attributed to the coherence energy transfer caused by the dipolar coupling of the <sup>13</sup>C nucleus to the directly coupled proton. Since then, transient oscillations have been used in a number of studies for studying spin dynamics [4,7–17], or as a basis for creating new pulse sequences for application in structural investigations [18–28].

SLF (separated local field) spectroscopy represents a family of very important 2D solid-state NMR experiments. In these experiments the heteronuclear dipolar coupling frequency is resolved from the chemical shift frequency, revealing the internuclear distance and orientation of the internuclear vector with respect to the direction of the applied magnetic field for a particular molecular site. Some of the techniques in this group use the transient oscillations which reflect dipole–dipole interactions of *S* spins with their immediate neighbors, so that suitable analysis can yield useful structural parameters [17–28]. In the first of these 2D experiments transient oscillations during the transfer of polarization from *I* spins to *S* spins have been studied, similar to a standard CP sequence [17,18]. However, Tekely et al.

\* Corresponding author. Fax: +64-9-373-7422.

E-mail address: [z.zujovic@auckland.ac.nz](mailto:z.zujovic@auckland.ac.nz) (Z.D. Žujović).

[25] have introduced a new concept in SLF spectroscopy, i.e., polarization inversion PI (Fig. 1a). This has improved the efficiency of the previous experiments leading to stronger transient oscillations (the amplitude of TO is twice that in standard CP).

The preparation period in the PI sequence ( $t_{cp}$ ) consists of the standard CP procedure. However, in the evolution period ( $t_1$ ), the phase of the proton spin-locking field is inverted, resulting in the polarization inversion of  $^{13}\text{C}$  magnetization. During that time interval, the heteronuclear dipolar interaction dominates, leading to amplitude modulation of the chemical shift information during the  $t_2$  period. The  $^{13}\text{C}$  magnetization as a function of the evolution time for different positions on the chemical shift-scale has oscillatory character and carries information about the local structure through the parameters available from transient oscillations.

One of the most important experiments for solid-state NMR of oriented membrane proteins, PISEMA, (Polarization Inversion Spin Exchange at the Magic Angle) is based on the measurement of dipolar couplings during the polarization inversion. The shortcoming of this very useful technique is its requirement for very high RF power due to the approximately ten times lower gyromagnetic ratio of  $^{15}\text{N}$  relative to that of  $^1\text{H}$ .

Thus, regardless of its wide application, the CP method (and all related experiments which use polarization transfer) cannot readily be applied to nuclei with low gyromagnetic ratios. In order to achieve the

Hartmann–Hahn condition, very high values of the RF power are required.

There are several proposed sequences that reduce the RF strength required for cross-polarization [30–32]. One of these is the time averaged precession frequency (TAPF) sequence [30], based on the TAPF of  $I$  spins. Alternating the phase of the  $I$  spin-locking field and using different duration times for phase alternating periods, one can control the precession frequency of the  $I$  spin isochromat around the spin locking field. This opens the possibility for a significant reduction of the  $S$  spin RF field strength required to cross-polarize a dilute spin system. This is very important in the case of biological samples where application of higher RF power (1 kW) is technically demanding and can denature the sample.

In the work described here we use a pulse sequence which yields transient oscillations even under strongly mismatched conditions, i.e., when the RF power in the  $S$  channel is significantly reduced, i.e., PI-TAPF. This gives the opportunity for the further development of new heteronuclear correlation pulse sequences, which can overcome the problem of the high RF power required for cross-polarization of nuclei with low  $\gamma$ . On the other hand, the transient oscillations can serve as a powerful tool to study theoretical and practical problems in cross-relaxation processes under strong mismatching. Thus, the dynamics of CP under the mismatch can be more easily understood.

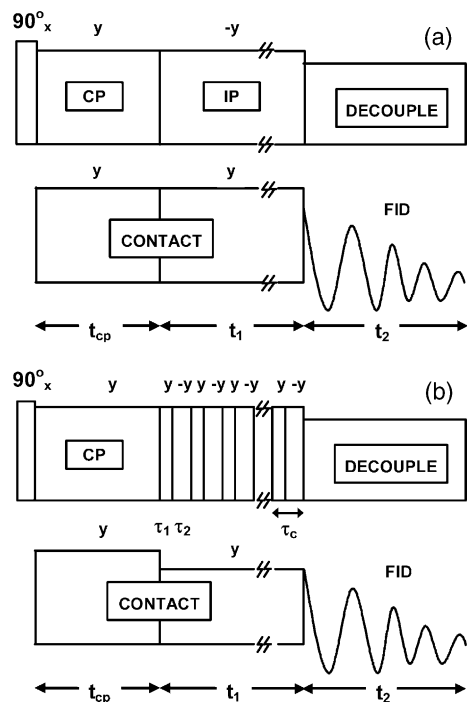


Fig. 1. Pulse sequence diagrams: (a) standard inversion polarization (PI) pulse sequence. (b) Inversion polarization + time averaged precession frequency (PI-TAPF) segment.

## 2. Results

### 2.1. Experimental results

In a powder pattern each spin packet corresponds to a particular set of orientations of the external field  $B_0$  with respect to the principal axis system of the chemical shift tensor. Since the powder pattern is inhomogeneous, the behavior of each spin packet can be studied separately. In particular since each orientation of the  $S$ -spin environment is characterized by its own transient oscillation frequency, the TO spectra can be interpreted in terms of the structural environment of the  $S$  spin, including its orientation with respect to the principal axes of the chemical shielding tensor.

A powder sample of ferrocene  $\text{Fe}(\text{C}_5\text{H}_5)_2$  was used for the experiments. This compound has been used in several studies of TO as a tool for designing new pulse sequences [19,29], or in the investigation of spin dynamics during CP [4,6,10,12,13,15]. Due to the fast molecular rotation of the  $\text{C}_5\text{H}_5$  ring about its  $\text{C}_5$  axis, its internal homonuclear and heteronuclear interactions are scaled by a factor of 2, while the interactions with adjacent rings are significantly reduced. The heteronuclear  $^1\text{H}$ - $^{13}\text{C}$  ( $I$ - $S$ ) interaction exceeds the vicinal  $^1\text{H}$ - $^1\text{H}$

interactions by a factor 3.7, [29] leading to a virtually isolated two-spin system with an oscillatory dependence of  $S$  magnetization on contact time characterized by

$$S(t_1) = -1 + \exp(-R_{df}t_1) + \exp[-0.5(R_{dp} + 2R_{df})t_1] \times \cos\left(\frac{\gamma_H\gamma_C\hbar}{8\pi r_{IS}^3}(3\cos^2\theta^{IS} - 1)t_1\right), \quad (1)$$

where  $R_{dp}$  and  $R_{df}$  are orientation dependent spin–diffusion rates of a particular spin  $I$  and  $\theta^{IS}$  is the angle between the internuclear vector of the  $I$ – $S$  spin pair and the static magnetic field.

The PI-TAPF experiment is shown in Fig. 1b. The basic principle used during the depolarization (or evolution) period is the segmentation applied in the standard TAPF sequence. Alternating the phase of the  $I$  spin-locking field with different periods  $\tau_1$  and  $\tau_2$  allows a significant reduction of the RF field strength in the  $S$  channel. The scaling factor of the RF field is limited by the correlation time of the dipolar fluctuation in the rotating frame,  $t_c$ . It can take any value as long as  $\tau_c \ll t_c$ , i.e.,

$$SC = \left| \frac{\tau_1 - \tau_2}{\tau_c} \right| \leq 1, \quad (2)$$

where  $\tau_c = \tau_1 + \tau_2$ .

Fig. 2 shows the  $^{13}\text{C}$  spectrum of a powder sample of ferrocene obtained with the PI sequence after 2  $\mu\text{s}$  of the evolution time, and the spectra obtained in the PI-TAPF depolarization experiments (see Fig. 1b) with time intervals  $\tau_1$  and  $\tau_2$  of 1 and 4  $\mu\text{s}$  ( $SC = 0.6$ ) as well as 2 and 3  $\mu\text{s}$  ( $SC = 0.2$ ), respectively. The fast molecular motion leads to an axially symmetric shielding tensor. The sharp peak located at 94.4 ppm originates from those  $^{13}\text{C}$  spins with the symmetry axis of the shielding tensor perpendicular to the external static magnetic field. The intensity of the peak at 94.4 ppm as a function of the polarization inversion time for the standard PI experiments (Fig. 1a) and for PI-TAPF with two different scaling factors (see Fig. 1b) is shown in Fig. 3.

All curves have an oscillatory character with similar amplitudes. The signal oscillates with attenuated amplitudes and different frequencies for each experiment. The transient oscillations are well reproduced by using Eq. (1) and taking into account the damping effect caused by spin–diffusion.

The dipolar frequencies obtained from the PI-TAPF experiments with different scaling factors after fitting the TO for the peak at 94.4 ppm are listed in Table 1. The values of  $A_{PI-TAPF}/A_{PI}$  listed in Table 1 represent the ratios of the amplitudes of TO obtained in PI-TAPF experiments to the amplitude of TO obtained in the PI experiment.

The Fourier transform of TO gives the Pake-like doublets (Fig. 4). The central (zero frequency) peak originates from spin a diffusion process which drives

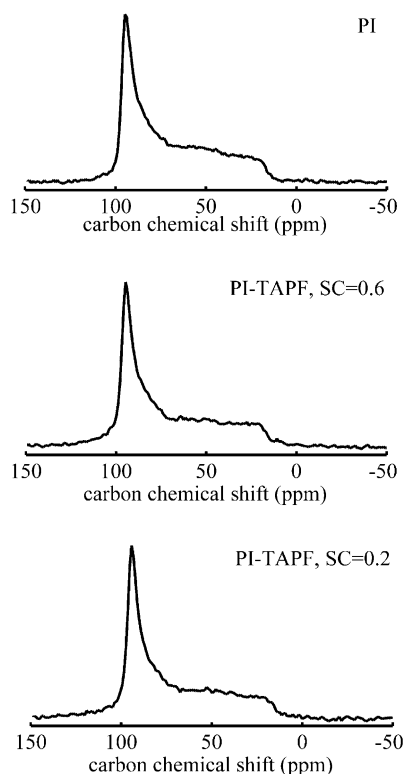


Fig. 2.  $^{13}\text{C}$  NMR spectra of the powder sample of ferrocene. The spectra were obtained at ambient temperature on a 300-MHz Bruker Avance spectrometer equipped with a 7-mm MAS probe operated in the static mode at 75.468 MHz  $^{13}\text{C}$  frequency. The number of  $t_1$  increments for both experiments was 32, with 24 scans for each  $t_1$  increment and a 25-s delay between scans. Contact time was 5 ms and sweep width 39.920 kHz. For the standard PI experiment (see Fig. 1a),  $^1\text{H}$  and  $^{13}\text{C}$  RF fields,  $\gamma B_{1I}/2\pi$  and  $\gamma B_{1S}/2\pi$ , were set to 59.524 kHz, satisfying the Hartmann–Hahn condition (asterisks). The first spectrum from the top is obtained from the standard PI experiment (see Fig. 1a), after 2  $\mu\text{s}$  evolution time. The second and third spectrum from the top are obtained from the PI-TAPF depolarization experiments (see Fig. 1b) with time intervals  $\tau_1$  and  $\tau_2$  of 1 and 4  $\mu\text{s}$  ( $SC = 0.6$ ) and 2 and 3  $\mu\text{s}$  ( $SC = 0.2$ ), respectively.  $^1\text{H}$  and  $^{13}\text{C}$  RF fields,  $\gamma B_{1I}/2\pi$  and  $\gamma B_{1S}/2\pi$ , were set to 59.524 kHz during the crosspolarization interval. During the PI-TAPF-depolarization period, according to the relative ratio of time intervals  $\tau_1$  and  $\tau_2$ , the  $^{13}\text{C}$  RF fields were reduced to 35.714 and 11.905 kHz, while  $\gamma B_{1I}/2\pi$  was kept at 59.514 kHz.

magnetization towards the final equilibrium state. The differences in frequency of TO for the PI and PI-TAPF experiments seen in Fig. 3 are reflected in the corresponding Fourier transform by the different line splitting between the intense singularities of the Pake-like powder pattern. Besides different splitting, there is significant narrowing of the lineshape singularities for PI-TAPF experiments with  $SC = 0.6$  (2.50 kHz) and  $SC = 0.2$  (2.00 kHz), relative to the PI experiment (3.35 kHz).

## 2.2. Simulations

Simulations of the experimental results are based on a numeric algorithm which has been described in detail

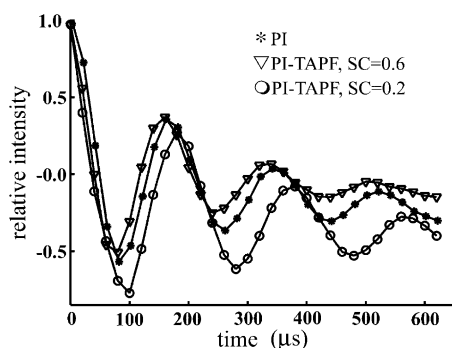


Fig. 3. Time dependence of the intensity of the peak at 94.4 ppm as a function of inversion polarization time and PI-TAPF inversion polarization time. The  $t_1$  increment was 20  $\mu\text{s}$ , starting from 2 and 0  $\mu\text{s}$  for PI and PI-TAPF depolarization experiments, respectively. The experimental conditions are the same as it is given in Fig. 2.

elsewhere [33]. It is based on a description of the cross-polarization process using single transition operators combined with rotational diffusion represented by a stationary Markov operator. It has been adapted to the PI condition by a suitable variation of the starting conditions and by introducing an additional exponential decay term  $\exp(-R_{\text{df}}t)$  corresponding to the spin diffusion process with a given rate constant  $R_{\text{df}}$  [34].

Simulation parameters account for a rapid rotational diffusion of the  $\text{C}_5\text{H}_5$  rings around their symmetry axes leading to partial averaging of the CSA tensor. With this motion being in the rapid limit, the sensitivity of the simulated results with respect to the rotational correlation time is very small, a standard value of  $\tau = 100$  ns has been used for the calculations.

The resulting shielding tensor is axially symmetric with  $\sigma_{\perp} = 95$  ppm and  $\sigma_{\parallel} = 20$  ppm, which is in general accordance with published data [35] and yields a line spectrum similar to the powder pattern shown in Fig. 2. The C–H vector is assumed to be perpendicular to the rotation axis [35] such that the dipolar coupling is partially averaged as well. Due to the orientation of the averaged dipolar interaction tensor, the resulting amplitude oscillations are strongly dependent on the signal position in the powder pattern. While the oscillation frequency is almost zero for the magic angle position (near 70 ppm), the frequencies for the 90° position (near

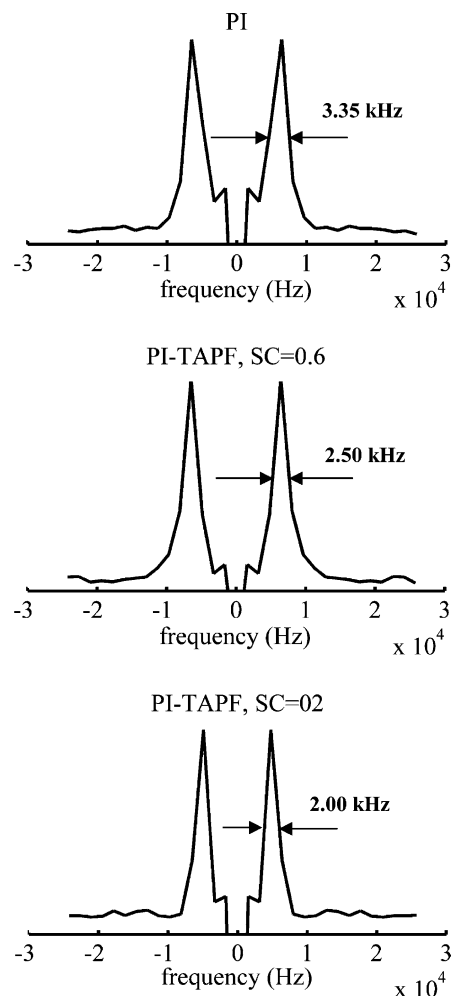


Fig. 4. Dipolar powder patterns obtained after FT of the transient oscillations shown in Fig. 3. The first spectrum from the top, (PI), was obtained using the standard PI experiment. The second and third spectra from the top are obtained from the PI-TAPF depolarization experiments (see Fig. 1b) with time intervals  $\tau_1$  and  $\tau_2$  of 1 and 4  $\mu\text{s}$  ( $\text{SC} = 0.6$ ) and 2 and 3  $\mu\text{s}$  ( $\text{SC} = 0.2$ ), respectively. The experimental conditions are the same as in Fig. 2.

95 ppm) and the 0° position (near 20 ppm) are significant and show a 1:2 relation.

With the dipolar coupling constant set to  $D_{\text{IS}} = 25.3 \text{ kHz} \cdot (1 - 3 \cos^2 \theta^{\text{IS}})$ , the oscillation frequency observed for the PI experiment as well as the frequency

Table 1

$^{13}\text{C}$  RF field strengths, dipolar frequencies obtained by fitting the TO, and the values  $A_{\text{PI-TAPF}}/A_{\text{PI}}$  which represent the ratios of the amplitudes of TO obtained in PI-TAPF experiments to the amplitude of TO obtained in PI experiment

Scaling factor, SC	RF field strength in carbon channel (kHz)	Dipolar frequency (kHz)	$A_{\text{PI-TAPF}}/A_{\text{PI}}$
0.8	47.62	5.88	1.02
0.6	35.71	6.08	0.97
0.5	29.76	5.69	0.99
0.4	23.81	5.84	0.92
0.2	11.90	5.32	0.96

shifts for the PI-TAPF experiments are well reproduced (Fig. 3). For standard PI experiments the signal near 95 ppm oscillates with a frequency of 6.000 kHz. The frequency for the PI-TAPF experiment with 40% (SC=0.6) RF power attenuation is 5.860 kHz. The frequency for the experiment with 80% (SC=0.2) RF power attenuation is 5.390 kHz. There is a difference in frequency (about 200 Hz) between the experimental and simulated data for the PI and PI-TAPF (SC=0.6) that can still lie within the experimental errors.

### 3. Discussion

For an RF field of 30 kHz theoretical investigation suggests that when the mismatching is 5 kHz (17%), the maximum amplitude is diminished by about 14% compared to HH conditions. However, in the case of the powder sample, for the same mismatching, the maximum amplitude of exchange is only 34% compared to the amplitude of single orientation for the Hartmann–Hahn matching condition [36,37]. The previous experimental data [13] for depolarization behavior during polarization inversion show that the frequency of the transient oscillations obtained from the peak at 94.4 ppm in the powder sample of ferrocene increases from about 6.0 kHz, for the Hartmann–Hahn matching conditions, to about 8.3 kHz under mismatched conditions ( $\omega_{II} = \gamma_I B_{II}/2\pi = 57$  kHz and  $\omega_{IS} = \gamma_{IS} B_{IS}/2\pi = 51$  kHz), according to the well-known equation [10] given by

$$\omega_e = [(\omega_{IS} - \omega_{II})^2 + d^2]^{1/2}. \quad (3)$$

The dependence of the TO frequency on mismatching is also given in the paper of Levitt et al. [4]. The frequency, which corresponds to the heteronuclear dipolar interaction, has a minimum at the Hartmann–Hahn match. Away from the matching condition, the frequency of the TO is higher.

The overall lineshape (see Fig. 2) also depends on SC and on the RF power applied during the experiment, although the differences among the spectra obtained from PI and PI-TAPF experiments are not so significant.

The differences of the TO frequencies observed in our experimental and simulated data (Figs. 3 and 5) suggest that the introduction of the fast phase alternation of the *I* spin-locking field could produce averaging of the heteronuclear dipolar interaction and scales the TO frequency. However, the same frequency scaling as in PI-TAPF experiment with SC=0.2 is obtained in the standard PI experiment (not shown) with the RF field strength of 11.905 kHz in both the *S* and the *I* channels. Although this PI experiment due to the same RF fields in both channels (11.905 kHz) cannot be directly compared to the PI-TAPF (59.524 kHz in *I* and 11.905 kHz in *S* channel), the same dipolar frequency ( $\approx 5.300$  kHz)

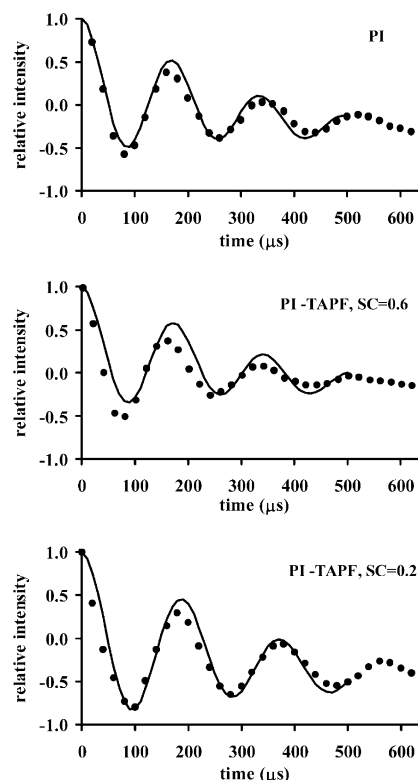


Fig. 5. Time dependence of the intensity of the peak at 94.4 ppm as a function of inversion polarization time PI (top) and PI-TAPF experiments with time intervals  $\tau_1$  and  $\tau_2$  of 1 and 4  $\mu$ s (SC=0.6, center) and 2 and 3  $\mu$ s (SC=0.2, bottom). All experimental data represented by dots are fitted with transient oscillatory curves obtained from numerical simulation (see text) of corresponding experiments with the same conditions as in Fig. 2.

in both experiments implies that reduction of the RF field strength in the *I* channel can cause frequency scaling, as well as phase alternation during the TAPF segment.

It is also interesting that in the case of SC=0.6, the unmodulated magnetization (zero-frequency peak, see Fig. 3) is much smaller than in both PI, and PI-TAPF (SC=0.2) experiments, which implies slower spin diffusion. Further, there is significant narrowing of the lineshape singularities in both PI-TAPF experiments (SC=0.2, SC=0.6) (Fig. 4). This suggests slower decay of the oscillatory term (Eq. (1)) for PI-TAPF experiments in comparison to the PI experiment [38].

Simulations and experimental data suggest that TO frequencies and amplitudes depend on the relative ratio of  $\tau_1$  and  $\tau_2$  (different SC), on the duration of those intervals for the same SC factor, and on the overall RF power used in the experiment. The work which should reveal the mechanisms and parameters which influence the polarization transfer during the PI-TAPF segment is in progress.

Whilst there are differences between the TO frequencies obtained in standard PI and PI-TAPF

experiments, the oscillatory character is still obvious, and the variation of the amplitudes is much smaller as expected from the degree of mismatching. However, a rapid phase alternation of the proton spin-locking field could result in its averaging. Thus, the spin-locking field can become less efficient which leads to shortening of  $T_{1\rho}^H$  and deterioration of the spectral resolution [39]. Further, a very important factor in the PI-TAPF sequence is the time interval  $\tau_c = \tau_1 + \tau_2$ . This interval should be significantly shorter than the dipolar correlation time. Actually, what is the limit for the duration of this interval? For oriented crystalline linear polyethylene as a representative rigid organic solid with strong dipolar couplings and for a powder sample of L-alanine using MAS, the correlation times are 24 and 31  $\mu\text{s}$ , respectively. In this way, the duration of 5  $\mu\text{s}$  for  $\tau_c$  should be long enough for most pairs of heteronuclear spins [30].

The significant mismatching conditions and values of the TO frequencies and amplitudes obtained in the PI-TAPF experiments imply that different mechanisms drive the cross-relaxation process under mismatched conditions. Thus, the previous conclusions based on the behavior of the spin system during the mismatching in standard CP sequences cannot be applied in our case.

Under these circumstances, an understanding of the mechanism and a study of the dependencies of the cross-relaxation mechanism on different parameters in the PI-TAPF experiment demand detailed experimental and theoretical analysis. The implementation of the PI-TAPF sequence on a single crystal sample of L-alanine is in progress. This system has a strong dipolar interactions and a short dipolar correlation time (30  $\mu\text{s}$ ) which allows revealing the characteristics and limitations of this sequence.

This report shows that it is possible to observe oscillations even under the condition where the required power for the dilute spins is reduced by a factor of 5 (Fig. 3). The results presented here could be used to design low-power RF pulse sequences on power lossy and heat sensitive biological samples such as, for example, hydrated lipid bilayers. Thus, further investigations will be aimed at the application of this method to 2D SLF experiments.

Combining the standard CP and PI-TAPF cross-relaxation schemes offers a powerful tool for experimental and theoretical investigations of crosspolarization dynamics and molecular motions under strong mismatching.

## References

- [1] A. Pines, M.G. Gibby, J.S. Waugh, Proton-enhanced NMR of dilute spins in solids, *J. Chem. Phys.* 59 (1973) 569–590.
- [2] R.R. Ernst, G. Bodenhausen, A. Wokaun, *Principles of Nuclear Magnetic Resonance in One and Two Dimensions*, Clarendon Press, Oxford, 1987.
- [3] M. Mehring, *High Resolution NMR in Solids*, Springer, New York, 1983.
- [4] M.H. Levitt, D. Suter, R.R. Ernst, Spin dynamics and thermodynamics in solid state NMR cross-polarization, *J. Chem. Phys.* 84 (1986) 4243–4255.
- [5] X. Wu, S. Zhang, X. Wu, Two stage feature of Hartmann–Hahn cross relaxation in magic-angle sample spinning, *Phys. Rev. Ser. B* 37 (1988) 9827–9829.
- [6] L. Müller, A. Kumar, T. Baumann, R.R. Ernst, *Phys. Rev. Lett.* 32 (1974) 1402–1406.
- [7] Z. Gan, Spin dynamics of polarization inversion spin exchange at the magic angle in multiple spin system, *J. Magn. Reson.* 143 (2000) 136–143.
- [8] T.N. Venkatraman, N. Sinha, K.V. Ramanathan, Cross-polarization from the dipolar reservoir under the mismatched Hartman–Hahn condition, *J. Magn. Reson.* 157 (2002) 137–140.
- [9] X. Wu, S. Zhang, Selective polarization inversion and depolarization of  $^{13}\text{C}$  in cross relaxation in NMR, *Chem. Phys. Lett.* 156 (1989) 79–81.
- [10] S. Zhang, B.H. Meier, S. Appelt, M. Mehring, R.R. Ernst, Transient oscillations in phase switched cross-polarization experiments, *J. Magn. Reson. Ser. A* 101 (1993) 60–66.
- [11] S. Zhang, C.L. Czekaj, W.T. Ford, Enhancement of polarization transfer under high-speed MAS using a quasi-adiabatic cross-polarization sequence, *J. Magn. Reson. Ser. A* 111 (1994) 87–92.
- [12] D. Sakellariou, P. Hodgkinson, S. Hediger, L. Emsley, Experimental observation of periodic quasi-equilibria in solid-state NMR, *Chem. Phys. Lett.* 308 (1999) 381–389.
- [13] X. Wu, K.W. Zilm, Heterogeneity of cross relaxation in solid state NMR, *J. Magn. Reson.* 93 (1991) 265–278.
- [14] D. Sakellariou, P. Hodgkinson, L. Emsley, Quasi-equilibria in solid-state NMR, *Chem. Phys. Lett.* 293 (1998) 110–118.
- [15] S. Zhang, Quasi-adiabatic polarization transfer in solid-state NMR, *J. Magn. Reson. Ser. A* 110 (1994) 73–76.
- [16] A. Naito, C.A. McDowell, Anisotropic behavior of the  $^{13}\text{C}$  nuclear spin dynamics in a single crystal of L-alanine, *J. Chem. Phys.* 84 (1986) 4181–4185.
- [17] R.K. Hester, V.R. Cross, L.L. Ackerman, J.S. Waugh, Resolved dipolar coupling spectra of dilute nuclear spins in solids, *Phys. Rev. Lett.* 34 (1975) 993–995.
- [18] R.K. Hester, V.R. Cross, L.L. Ackerman, J.S. Waugh, Structure determination by dipolar coupling measurements of dilute nuclear spins in a polycrystalline solid, *J. Chem. Phys.* 63 (1975) 3606–3608.
- [19] P. Palmas, P. Tekely, D. Canet, Local-field measurements on powder samples from polarization inversion of the rare-spin magnetization, *J. Magn. Reson. Ser. A* 104 (1993) 26–36.
- [20] A. Ramamoorthy, C.H. Wu, S.J. Opella, Experimental aspects of multidimensional solid-state NMR correlation spectroscopy, *J. Magn. Reson.* 140 (1999) 131–140.
- [21] C.H. Wu, A. Ramamoorthy, S.J. Opella, High resolution heteronuclear dipolar solid-state NMR spectroscopy, *J. Magn. Reson.* 109 (1994) 270–272.
- [22] A. Ramamoorthy, C.H. Wu, S.J. Opella, Three-dimensional solid state NMR experiment that correlates the chemical shift and dipolar coupling frequencies of two heteronuclei, *J. Magn. Reson. Ser. B* 107 (1995) 88–90.
- [23] A. Ramamoorthy, L.M. Gierasch, S.J. Opella, Four dimensional solid-state NMR experiment that correlates the chemical shift and dipolar coupling frequencies of two heteronuclei with the exchange of dilute spin magnetization, *J. Magn. Reson. Ser. B* 107 (1995) 112–116.
- [24] F. Tian, Z. Song, T.A. Cross, Orientational constraints derived from hydrated powder samples by two-dimensional PISEMA, *J. Magn. Reson.* 135 (1998) 227–231.

- [25] P. Tekely, F. Montigny, D. Canet, J.J. Delpuech, High resolution dipolar NMR spectra in rotating solids from depolarization of the rare spin magnetization, *Chem. Phys. Lett.* 175 (1990) 401–406.
- [26] E. Vinogradov, P.K. Madhu, S. Vega, High-resolution proton solid-state NMR spectroscopy by phase-modulated Lee–Goldburg experiment, *Chem. Phys. Lett.* 314 (1999) 443–450.
- [27] R. Pratima, K.V. Ramanathan, The application to liquid crystals of transient oscillations in cross polarization experiments, *J. Magn. Reson. Ser. A* 118 (1996) 7–10.
- [28] N. Sinha, K.V. Ramanathan, Use of polarization inversion for resolution of small dipolar couplings in SLF-2D NMR experiments—an application to liquid crystals, *Chem. Phys. Lett.* 332 (2000) 125–130.
- [29] S. Zhang, B.H. Meier, R.R. Ernst, Mismatch-compensated cross polarization. W-MOIST, an improved pulse scheme, *J. Magn. Reson. Ser. A* 108 (1994) 30–37.
- [30] K. Takegoshi, C.A. McDowell, Cross polarization using a time averaged precession frequency. A simple technique to reduce radiofrequency power requirements for magnetization transfer experiments in solids, *J. Magn. Reson.* 67 (1986) 356–361.
- [31] A. Bax, B.L. Hawkins, G.E. Maciel, Off-resonance cross-polarization: a technique to reduce rf power requirements for magnetization transfer experiments in solids, *J. Magn. Reson.* 59 (1984) 530–535.
- [32] S.C. Shekar, D. Lee, A. Ramamoorthy, An experimental strategy to dramatically reduce RF power used in cross polarization solid-state NMR spectroscopy, *J. Am. Chem. Soc.* 123 (2001) 7467–7468.
- [33] C. Mayer, Calculation of cross-polarization spectra influenced by slow molecular tumbling, *J. Magn. Reson.* 145 (2000) 216–229.
- [34] J. Hirschinger, M. Hervé, *Solid State Nucl. Magn. Reson.* 3 (1994) 121–135.
- [35] K.J. Hallock, D.K. Lee, A. Ramamoorthy, *Chem. Phys. Lett.* 302 (1999) 175–180.
- [36] S.C. Shekar, D. Lee, A. Ramamoorthy, Chemical shift anisotropy and offset effects in cross polarization solid-state NMR spectroscopy, *J. Magn. Reson.* 157 (2002) 223–234.
- [37] S.C. Shekar, A. Ramamoorthy, The unitary evolution operator for cross-polarization schemes in NMR, *Chem. Phys. Lett.* 342 (2001) 127–134.
- [38] P. Bertani, J. Raya, P. Reinheimer, R. Gougeon, L. Delmotte, J. Hirschinger,  $^{19}\text{F}/^{29}\text{Si}$  distance determination in fluoride-containing octadecyl by Hartmann–Hahn cross-polarization under fast magic angle spinning, *J. Magn. Reson.* 13 (1999) 219–229.
- [39] R. Fu, C. Tian, T.A. Cross, NMR spin locking of proton magnetization under a frequency-switched Lee–Goldburg pulse sequence, *J. Magn. Reson.* 154 (2002) 130–135.